

Pulsed field gradient n.m.r. diffusion measurements on electrolyte solutions containing LiCF_3SO_3

M.J. Williamson, J.P. Southall, H.V.St.A. Hubbard, G.R. Davies, I.M. Ward*

IRC in Polymer Science and Technology, University of Leeds, Leeds LS2 9JT, UK

Received 25 May 1998; accepted 22 August 1998

Abstract

The pulsed field gradient spin echo technique has been used to measure the self-diffusion coefficients of ^7Li , ^{19}F and protons in two electrolyte solutions, based on LiCF_3SO_3 in either tetraglyme or N,N-dimethylformamide, respectively. In addition, the ionic conductivities were determined by ac conductivity measurements and the viscosities with an Ostwald viscometer. Predicted values for the ionic conductivity were obtained from the n.m.r. diffusivities using the Nernst–Einstein equation and compared with those from direct measurements, to provide estimates of the degree of ionic association as a function of temperature and salt concentration. The possible correlations between solution viscosity and the self-diffusion coefficients of the ions were explored on the basis of the Stokes–Einstein equation. Finally, the results were considered in the light of previously reported Raman spectroscopy measurements and in terms of the Walden product of the molal conductivity and viscosity of the electrolyte. © 1999 Elsevier Science Ltd. All rights reserved.

Keywords: Pulsed field gradient n.m.r.; Liquid electrolyte; Ionic association

1. Introduction

Recent research on ionically conducting polymers at Leeds University has concentrated on the development of polymer gel electrolytes [1,2]. It has been shown that polyvinylidene fluoride (PVDF) can be dissolved in an electrolyte solution at high temperatures to form a thermoreversible gel with excellent mechanical properties on cooling. Furthermore, for selected electrolyte solutions, notably lithium trifluoromethanesulphonate (lithium ‘triflate’ (LiT), LiCF_3SO_3) in tetraglyme (TG) or N,N-dimethylformamide (DMF), very satisfactory levels of ionic conductivity were obtained (approx. 10^{-3} Scm^{-1} at room temperature).

N.m.r. pulsed field gradient spin echo measurements offer the opportunity to obtain quantitative measurements of ionic diffusion coefficients to compare with measurements of ionic conductivity and hence gain understanding of the degree of ionic association and its variation with salt concentration and temperature.

In this paper the self-diffusion coefficients of ^7Li , ^{19}F and protons in the two liquid electrolyte systems are compared and the relationship between the measured ionic conductivity and that predicted from the diffusion coefficients of the

^7Li and ^{19}F nuclei on the basis of the Nernst–Einstein equation. Next, the possible correlation between the measured macroscopic viscosity of the electrolyte solutions and the self-diffusion coefficients of the ions and protons is considered by application of the Stokes–Einstein equation, making the simplistic assumption that the macroscopic viscosity can replace the microscopic viscosity experienced by the diffusing ions and solvent molecules. Finally, the implications of the n.m.r. results for understanding the effect of salt concentration on the molal conductivity are considered in the light of the Walden product and Raman spectroscopy measurements.

2. Experimental

2.1. Preparation of samples

Lithium triflate was obtained from Aldrich and dried in a vacuum oven at 130°C for 48 h prior to dissolution in the solvents. Tetraglyme and DMF were also obtained from Aldrich and stored over a molecular sieve prior to use.

Liquid electrolytes in the molality range, $m = 0.23$ – 1.88 mol.kg^{-1} (O:Li = 100:1 to 12:1) for TG and $m = 0.14$ – 4.56 mol.kg^{-1} (O:Li = 100:1 to 3:1) for DMF were prepared by dissolving LiT in the solvents. All sample preparation took place in an oxygen-free nitrogen

* Corresponding author. Tel.: + 44-113-233-3808; fax: + 44-113-233-3809.

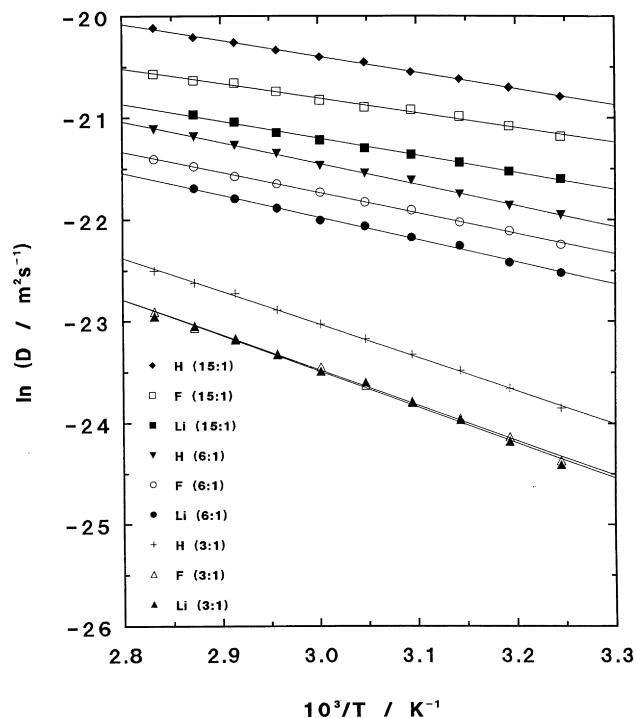


Fig. 1. Comparison of proton, lithium and fluorine diffusion coefficients in DMF/LiT liquid electrolytes. The solid lines represent the best fit lines of the data to Eq. (1).

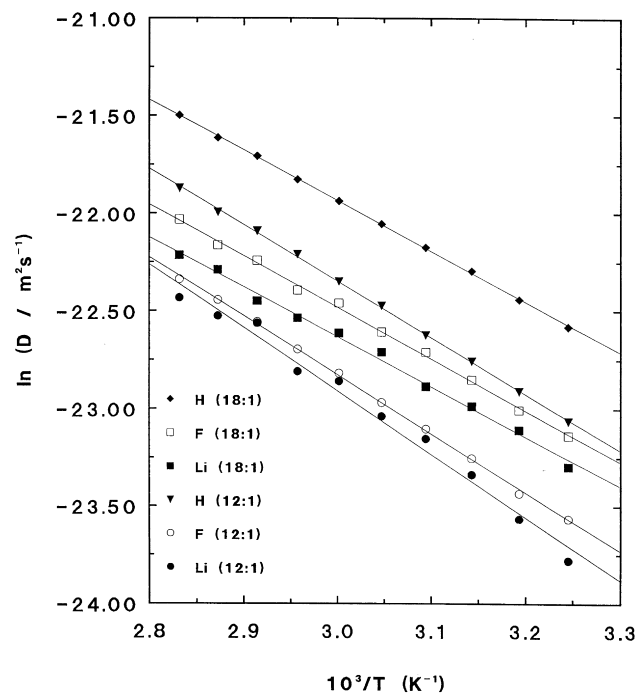


Fig. 2. Comparison of proton, lithium and fluorine diffusion coefficients in TG/LiT liquid electrolytes at salt concentrations of 12:1 and 18:1. The solid lines represent the best fit lines of the data to Eq. (1).

atmosphere in a glove box. For the n.m.r. measurements, the liquid electrolytes were pipetted into 7-mm diameter n.m.r. sample tubes to a depth of approximately 10 mm. The samples were then subjected to several freeze–pump–thaw cycles to remove any dissolved oxygen before the tubes were sealed.

2.2. N.m.r. measurements

The nuclei selective nature of n.m.r. has been used to obtain separate measurements of self-diffusion coefficients for solvent molecules (^1H measurements), Li^+ cations (^7Li measurements) and CF_3SO_3^- anions (^{19}F measurements) in the liquid electrolytes by use of the pulsed field gradient (PFG) spin echo technique [3].

This technique involves the application of a $\pi/2(+x)$ rf pulse at time zero, followed by a $\pi(+y)$ pulse at time τ so that a spin echo is formed at time 2τ . In addition, a square shaped field gradient pulse of magnitude $+G$ and duration δ is applied between the two rf pulses and a second identical gradient pulse is applied following the $\pi(+y)$ pulse at a time Δ after the first one. The echo amplitude is attenuated by an amount dependent on how much the position of the spins has changed by the process of self-diffusion in the time interval Δ . In practice it is found that unattenuated echoes are more stable if a very small field gradient, G_0 , is applied rather than no field gradient at all. It can then be shown that the attenuation of the echo amplitude is given by:

$$R = \frac{M(G)}{M(G_0)} = \exp\left\{-\gamma^2 D(G^2 - G_0^2)\delta^2\left(\Delta - \frac{\delta}{3}\right)\right\} \quad (1)$$

where D is the self-diffusion coefficient and γ is the gyromagnetic ratio of the spin.

Typically values of $\delta = 3$ ms, $\Delta = 40$ ms and $\tau = 30$ ms were used and G could be controlled to 1 part in 4096 up to a maximum of 2 T m^{-1} . D is determined from the slope of a graph of $\ln R$ against $G^2 - G_0^2$. The field gradient coils were calibrated on a sample of distilled water at 35°C using the diffusion data reported by Mills [4].

The diffusion measurements were carried out at 5°C intervals in the temperature range 35 – 80°C using an extensively modified Bruker SXP-100 spectrometer with a resonance frequency of approximately 100.6 MHz for protons, 95.6 MHz for fluorine and 39.1 MHz for lithium. The measurements were undertaken with the aid of a commercial pulse programmer/data acquisition system run from a PC.

2.3. Viscosity measurements

Viscosity measurements were made using an Ostwald Viscometer immersed in a temperature-controlled water bath in the temperature range 0 – 80°C . In samples of sufficiently low viscosity, measurements were extended down to -20°C by using a bath which contained a mixture of acetone and solid carbon dioxide. The Viscometer was calibrated using a sample of distilled water using published data for the viscosity of water [5]. In this paper the results

Table 1
Summary of activation energies (in units of $\text{kJ}\cdot\text{mol}^{-1}$) for diffusion and fluidity processes for DMF/LiT liquid electrolytes

| O:Li | Diffusion coefficient | | | Fluidity |
|-------|-----------------------|----------|---------|----------|
| | Proton | Fluorine | Lithium | |
| 3:1 | 27.0 | 28.7 | 29.1 | 27.7 |
| 4:1 | 23.8 | 22.3 | 24.1 | 22.6 |
| 5:1 | 21.1 | 19.6 | 20.8 | 19.8 |
| 6:1 | 17.2 | 16.5 | 18.1 | 17.0 |
| 9:1 | 14.6 | 16.1 | 15.9 | 13.5 |
| 15:1 | 13.2 | 12.0 | 14.0 | 12.2 |
| 33:1 | 12.5 | — | — | 10.9 |
| 50:1 | 12.5 | — | — | 10.4 |
| 100:1 | 12.0 | — | — | 9.4 |
| DMF | 12.1 | — | — | 9.8 |

are presented in terms of the fluidities, where the fluidity ϕ is defined as reciprocal viscosity.

2.4. Conductivity measurements

The ionic conductivities of the liquid electrolytes were measured using a Schlumberger 1260 Impedance/gain-phase analyser (frequency range 1 Hz–400 kHz). The sample was contained in a modified Philips PW9550/60 conductivity cell and after degassing on a vacuum line, remained sealed during the experiment. The cell was immersed in a temperature-controlled bath containing a mixture of water and antifreeze and measurements were taken at 5°C intervals on a heating cycle in the temperature range -20 to $+80^\circ\text{C}$. Further details of the ionic conductivity experimental apparatus have previously been provided in reference [1].

3. Results and discussion

3.1. Proton, ^7Li and ^{19}F self-diffusion measurements

Fig. 1 and Fig. 2 show the variation with temperature of the self-diffusion coefficients for the solvent molecules,

Table 2
Summary of activation energies (in units of $\text{kJ}\cdot\text{mol}^{-1}$) for diffusion and fluidity processes for TG/LiT liquid electrolytes

| O:Li | Diffusion coefficient | | | Fluidity |
|-------|-----------------------|----------|---------|----------|
| | Proton | Fluorine | Lithium | |
| 12:1 | 24.0 | 25.0 | 27.0 | 21.9 |
| 15:1 | 22.0 | 22.9 | 24.9 | 20.5 |
| 18:1 | 21.5 | 21.9 | 21.2 | 18.1 |
| 24:1 | 20.7 | — | — | 18.3 |
| 30:1 | 19.4 | — | — | 16.6 |
| 40:1 | 19.0 | — | — | 16.4 |
| 60:1 | 18.1 | — | — | 15.6 |
| 100:1 | 17.6 | — | — | 15.6 |
| TG | 17.0 | — | — | 14.0 |

Li^+ ions and CF_3SO_3^- ions in the DMF/LiT and TG/LiT solutions, respectively, at selected salt concentrations. In each case the echo attenuation decayed exponentially with $G^2 - G_0^2$ as expected for a single diffusing species.

A similar pattern of behaviour can be discerned for both the polar solvent DMF and the less polar solvent TG. First, the diffusion coefficients for the solvent molecules are always greater than for the Li^+ and CF_3SO_3^- ions. Secondly, there is a close correspondence between the values of the lithium and fluorine diffusion coefficients with the fluorine values always greater than the lithium values, but becoming increasingly similar, in fact almost coincident, at the highest salt concentrations.

As suggested by Clericuzio et al. [6] for electrolyte solutions based on LiBF_4 , the fast diffusion coefficients observed for the solvent can be attributed to the fact that the n.m.r. measurements relate primarily to the larger number of solvent molecules which are not solvating the salt. The somewhat larger diffusion coefficients for the fluorine ions compared with the lithium ions is consistent with the view that some degree of association between the lithium ions and the solvent molecules is likely.

There are two possible explanations for the general observation that the fluorine and lithium diffusion coefficients become increasingly similar in value with increasing salt concentration. First, this could be due to an increase in ionic association so that many ions pair and effectively move as a single species. Secondly, this could be due to correlated motion of the ions at high salt concentrations as previously suggested by Boden et al. [7,8], on the basis of n.m.r. measurements on low molecular weight polyethylene glycols containing LiT.

Fig. 1 and Fig. 2 also show that the Arrhenius plots for the diffusion of each species at each salt concentration are essentially linear, which suggests thermally activated processes. Therefore the diffusion data have been fitted to the Arrhenius equation:

$$D = D_0 \exp\left[\frac{-E_D}{RT}\right] \quad (2)$$

The preexponential fitting parameter, D_0 , is found to increase with increasing salt concentration for each species in both liquid electrolytes, as do the activation energies, E_D , which are given in Table 1 for the DMF/LiT electrolytes and in Table 2 for the TG/LiT electrolytes. In both cases it can be seen that the activation energies for protons, fluorine and lithium ions are very similar despite there being significant differences in the actual values of diffusion coefficient. This may indicate that the mechanisms responsible for diffusion are similar for each species. For the DMF/LiT electrolytes, it appears that the activation energy for lithium is marginally greater than that for fluorine, which indicates a stronger association of the lithium cation to DMF molecules.

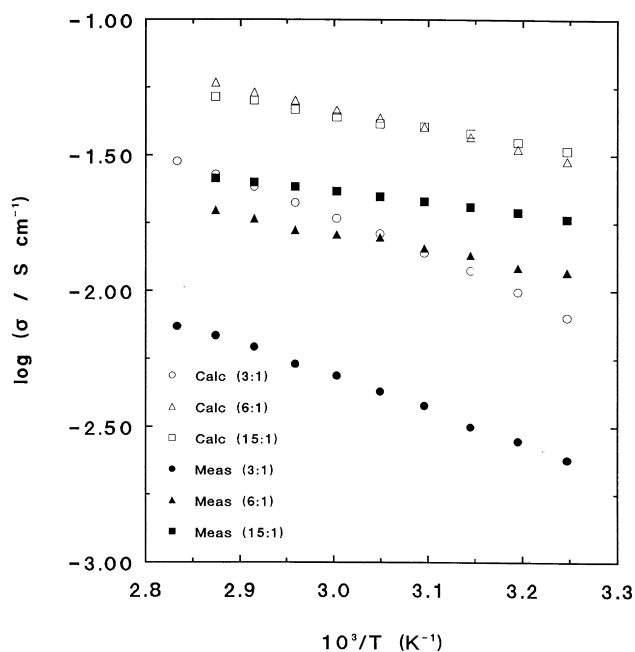


Fig. 3. Comparison of the measured ionic conductivity to the ionic conductivity calculated from the Nernst–Einstein equation using fluorine and lithium diffusion coefficients for DMF/LiT liquid electrolytes.

3.2. Mean displacements of species during diffusion experiments

The measurement of diffusion coefficients allows us to calculate the mean displacements of diffusing species on different experimental timescales. Using a random walk

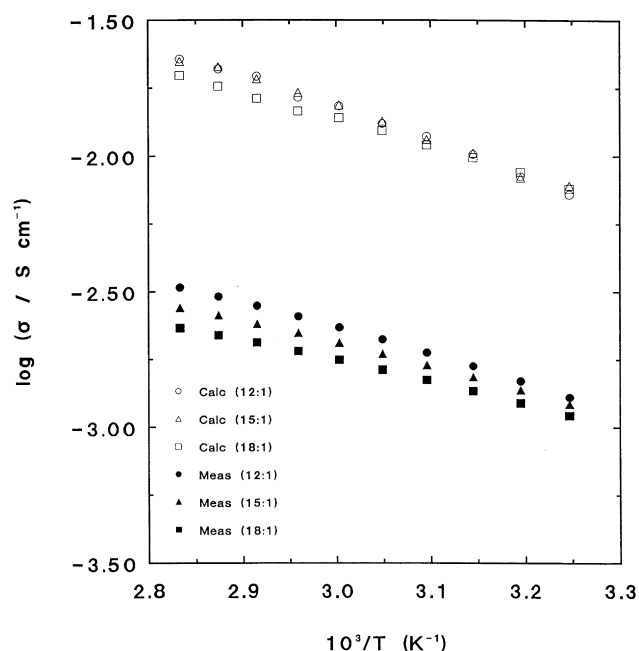


Fig. 4. Comparison of the measured ionic conductivity to the ionic conductivity calculated from the Nernst–Einstein equation using fluorine and lithium diffusion coefficients for TG/LiT liquid electrolytes.

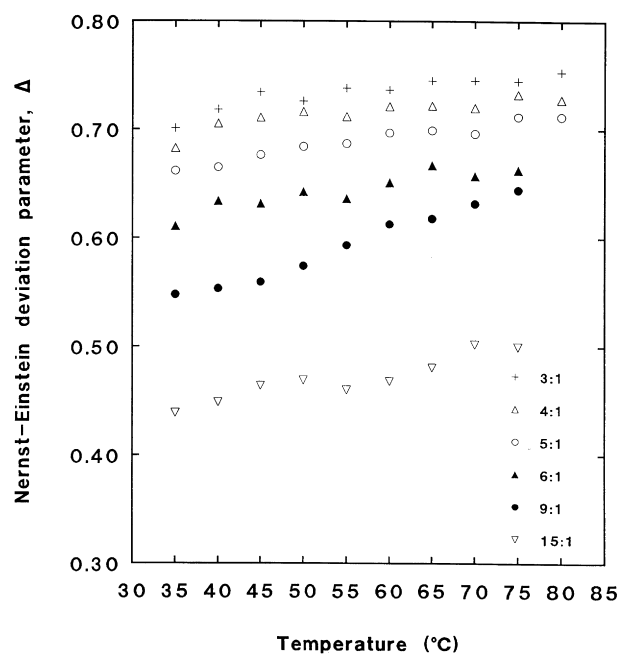


Fig. 5. Behaviour of the Nernst–Einstein deviation parameter with salt concentration and temperature for DMF/LiT liquid electrolytes.

argument [9], it can be shown that the mean displacement, d , of a diffusing particle in a time t can be approximated as:

$$d = \sqrt{\overline{\Delta d^2}} = \sqrt{6Dt} \quad (3)$$

where $\overline{\Delta d^2}$ is the mean square displacement and D is the diffusion coefficient. The timescale that should be substituted into Eq. (3) for the diffusion experiments is the diffusion time of the PFG n.m.r. experiments, given by $t = \Delta - \delta/3$, which is of the order of 40 ms.

Displacements in the range 3.2–27 μm and 4.8–15 μm are calculated for DMF and TG molecules, respectively, with the larger displacements occurring at higher temperatures and lower salt concentrations. The displacements of Li^+ and CF_3SO_3^- ions in both electrolytes are slightly smaller than those of solvent molecules, but are still of the order of a few microns.

3.3. Ion mobility and ionic conductivity: use of Nernst–Einstein equation

A calculated route to the ionic conductivity can be derived from the Nernst–Einstein equation

$$\sigma = \frac{nq^2}{kT} [D(\text{Li}^+) + D(\text{CF}_3\text{SO}_3^-)] \quad (4)$$

where n is the number of anions and/or cations per unit volume of solution, q is the charge on each ion and $D(\text{Li}^+)$ and $D(\text{CF}_3\text{SO}_3^-)$ are the diffusion coefficients of the cation and anion, respectively. Because the n.m.r. technique does not distinguish between a free ion and an ion pair or correlated motion of anions and cations in neutral pairs or clusters, the ionic conductivity, σ_{calc} , calculated from the

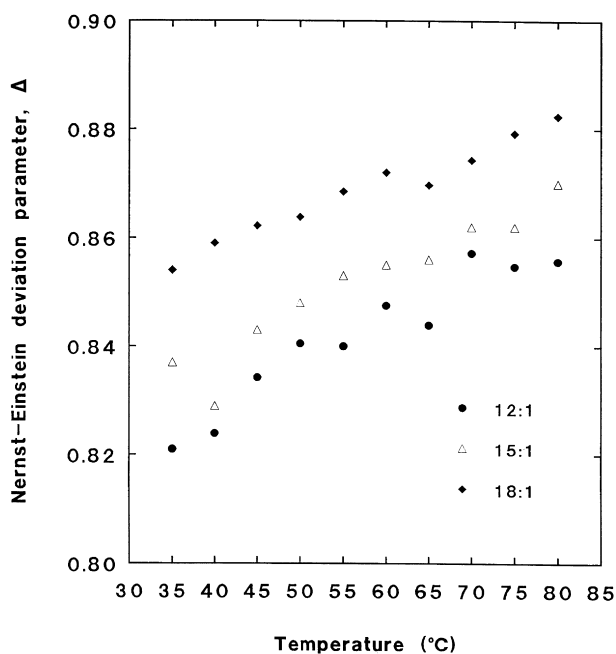


Fig. 6. Behaviour of the Nernst–Einstein deviation parameter with salt concentration and temperature for TG/LiT liquid electrolytes.

n.m.r. data as the basis of Eq. (4) is often found [7,8] to be higher than that measured directly, σ_{meas} . By defining Δ by:

$$\sigma_{\text{meas}} = \sigma_{\text{calc}}(1 - \Delta) \quad (5)$$

Δ is a parameter which is a measure of ionic association, taking a value of $\Delta = 0$ for an electrolyte in which the salt is fully dissociated, with $\Delta \rightarrow 1$ for complete association of ions in neutral pairs or clusters.

In Fig. 3, the measured conductivity [10] for DMF/LiT liquid electrolytes at three salt concentrations over the temperature range used in the n.m.r. diffusion measurements is shown, together with the conductivity calculated from the Nernst–Einstein equation from the measured lithium and fluorine diffusion coefficients. An equivalent plot for TG/LiT liquid electrolytes is shown in Fig. 4. In both cases, the plots show a clear difference between the measured and calculated conductivity for each salt concentration, with the implication being that the Nernst–Einstein relation does not hold for either DMF/LiT or TG/LiT liquid electrolytes at these high levels of salt content. Therefore, to obtain a quantitative measure of ionic association and how this changes with salt concentration and temperature, Eq. (5) was used to calculate the discrepancy factor Δ . The variation of Δ with salt concentration and temperature is shown in Fig. 5 for DMF/LiT electrolytes and in Fig. 6 for TG/LiT electrolytes.

In the case of the DMF/LiT electrolytes, the values of Δ vary from 0.43 to 0.75, depending on the salt concentration and temperature. Inspection of Fig. 5 indicates an increase in the value of Δ as the temperature increases and as the salt concentration is increased. This implies that there is

increased association of the ions under these conditions that lead to a greater proportion of currentless diffusion.

For the TG/LiT electrolytes, values of Δ in the range 0.8–0.9 are obtained, depending on the salt concentration and temperature, indicating a large degree of currentless diffusion in the TG/LiT electrolytes at these high levels of salt concentration. This range of values for Δ is in good agreement with values calculated on other related systems. Cruickshank [11] reported values of Δ of the order of 0.82 for end-esterified PEG with a molecular weight of 200, salted with lithium triflate to a concentration of O:Li = 12:1. A value of $\Delta = 0.87$ has been reported for a LiBF₄/TG system at 27°C salted to a concentration of 4.2% salt content by weight [6].

Fig. 6 shows that the value of Δ and hence the proportion of currentless diffusion for the TG/LiT electrolytes increases as the temperature increases and also as the salt concentration falls. This is in good agreement with the trends reported by Cruickshank in his studies of low molecular weight PEGs salted with LiT [11].

The calculations of Δ highlight both similarities and differences in the behaviour of ionic association in DMF/LiT and TG/LiT liquid electrolytes. For both electrolyte systems, the trends in Δ suggest that ionic association is increasing with increasing temperature. However, the trends in Δ with salt concentration suggest that ionic association is increasing with increasing salt concentration for the DMF/LiT electrolytes, but is decreasing with increasing salt concentration for the TG/LiT electrolytes.

The trend of increasing ionic association with increasing temperature is somewhat counter intuitive—one might expect the increasing thermal energy of the electrolyte to disrupt the formation of ion pairs. However, this is behaviour that has been widely observed in other electrolyte systems [12–16], and can be related to thermodynamic effects [17,18]. In the model of Nitzan and Olender [17] in which the dissolved salt dissociates to free ions according to $MA = M^+ + A^-$, the free energy of formation, ΔG^0 , is given by $\Delta G^0 = \Delta H^0 - T \Delta S^0$. The equilibrium constant K , which relates to the experimentally determined free and associated ion concentrations, is given by $K = \exp(-\Delta G^0/RT)$. Assuming that ΔH^0 and ΔS^0 do not depend on temperature, the change in K with temperature is given by $d(\ln K)/dt = \Delta H^0/RT^2$ and the temperature dependence of the observed change in ionic association is therefore determined by ΔH^0 . This enthalpy change includes an energy term ΔH_E associated with the salt dissociation reaction which is expected to be positive, but this is outweighed by a negative contribution to the enthalpy, $\Delta H_V = p\Delta V$ due to electrostriction with a decrease in volume accompanying ion solvation. Thus, an overall negative ΔH^0 leads to a decrease in free ion concentration with temperature, as observed. It has also been pointed out by Forsyth et al. [19] that the reduction in dielectric constant of a solvent with increasing temperature also favours the formation of ion pairs.

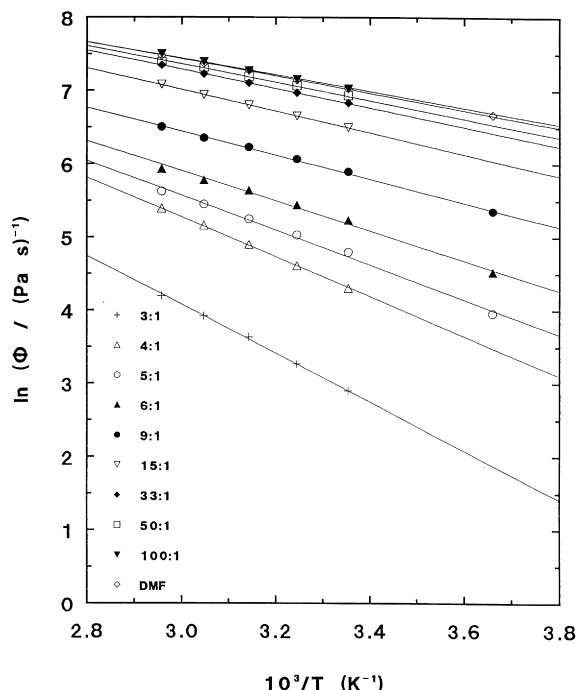


Fig. 7. Arrhenius plot of the fluidities of DMF/LiT liquid electrolytes. The solid lines represent the best fit lines of the data to Eq. (6).

Prior to any attempt to explain the fall in Δ with increasing salt concentration in the TG/LiT electrolytes, it is first worth considering the behaviour of the molal conductivity, $\Lambda = \sigma/m$, for electrolytes where the solvent has a low dielectric constant [20,21] or more specifically, where the solvent is a low molecular weight polyether [22,23]. In the case of low molecular weight polyether electrolytes, the molal conductivity was found to fall with increasing salt concentration at low salt concentrations, before passing through a minimum and starting to rise again. At higher salt concentrations Λ passed through a broad maximum before falling away with further increases in the salt concentration. This type of behaviour of Λ with salt concentration has also been observed by Hall et al. [24] in Leeds in their studies of LiClO_4 and LiBF_4 in tetraglyme.

The initial fall in Λ with increasing salt concentration was attributed to the formation of ion pairs and the final fall to a rapid increase in the viscosity at high salt concentrations. There have been a number of proposals put forward to explain the rise in Λ at intermediate salt concentrations. The first proposal, by Fuoss and Kraus [25] was that the rise in Λ was due to the increased Coulombic forces between free ions and ion pairs as the salt concentration increased which resulted in the formation of charged ion triplets. It has also been suggested that the rise in Λ may be due to a re-dissociation of the ion pairs [23] owing to a rise in the dielectric constant of the polyether with increasing salt concentration [26].

A further possible explanation is that at high salt concentrations the electrolyte is better described as an ionic melt, in which small amounts of solvent have been dispersed. In an

ionic melt, conduction takes place when an ion diffuses into a vacancy. In this case the currentless diffusion is due to the correlated motion of ions, which occurs when a cation and anion simultaneously move into a vacancy of sufficient size to accommodate both ions [27], rather than being due to the formation of discrete uncharged ion pairs. Boden et al. [7,8] proposed that as the proportion of solvent in an ionic melt-like electrolyte is increased (i.e. as the salt concentration is reduced), the correlated motion increases because the increased amount of solvent serves to disrupt the symmetry of the Coulombic fields surrounding the ions.

Bruce and Vincent [28] suggested that it is likely that several mechanisms are responsible for the rise in molal conductivity observed for electrolytes with a low dielectric constant and concurred with Boden et al. [7,8] that at high levels of salt concentration these electrolytes are better described as ionic melts.

Examination of the plot of Λ against salt concentration for the TG/LiT electrolytes [10,29] indicates that for the salt concentrations for which values of Δ have been calculated from Eq. (5), we are situated in the high salt concentration region where Λ is falling with increasing salt concentration due to the rapid increase in solution viscosity. However, the values of Δ suggest that the ionic association is continuing to decrease with increasing salt concentration in this region, suggesting that the mechanisms responsible for the rise in Λ at lower salt concentrations (whether they be the formation of ion triplets, re-dissociation of ions or trends towards ionic melt-like behaviour) are continuing to occur at higher salt concentrations, but are masked by the rapid increase in viscosity of the electrolytes in this region.

The increase in ionic association as the salt concentration increases for the DMF/LiT systems is consistent with the behaviour of 'strong' electrolytes [30]. In strong electrolytes the salt is fully ionized at all salt concentrations and a fall in molal conductivity with increasing salt concentration (which has been observed for the DMF/LiT electrolytes [10,29]) is due to the formation of contact and/or non-contact (solvent-shared or solvent-separated) [31] ion pairs, thus reducing the number of potential conducting species in the electrolytes. At higher salt concentrations reductions in the mobility of the ions as the viscosity rapidly increases will, as in the case of low molecular weight polyether electrolytes, also serve to reduce the molal conductivity with increasing salt concentration.

3.4. Correlations between ion diffusion and viscosity measurements: use of Stokes–Einstein equation

A route to obtaining a molecular understanding of the ionic conductivity is to explore the relationship between the measured macroscopic viscosity and the diffusion of the ions and solvent molecules through use of the Stokes–Einstein equation:

$$D = \frac{kT\phi}{6\pi a} \quad (6)$$

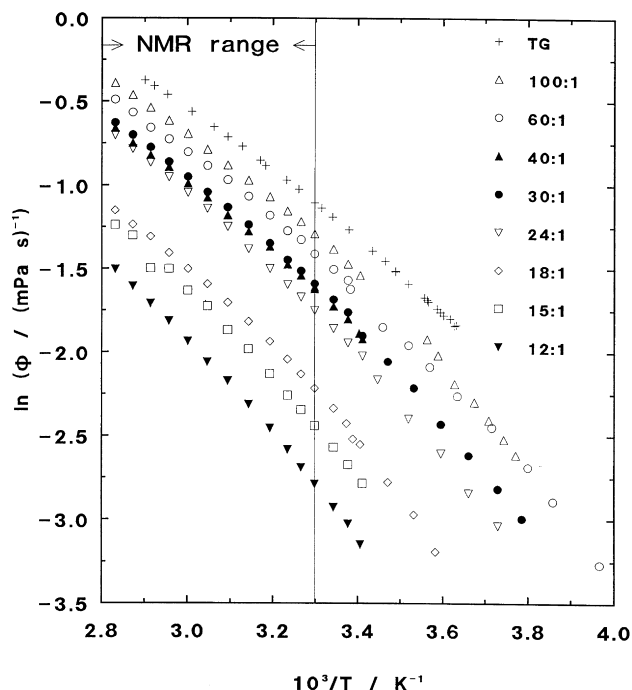


Fig. 8. Arrhenius plot of the fluidities of TG/LiT liquid electrolytes. The temperature range over which the n.m.r. measurements were taken is also indicated.

which relates the fluidity ϕ to the diffusion coefficient D and the effective radius, a , of the diffusing species.

The viscosities of the DMF/LiT liquid electrolytes were measured at six temperatures in the range 0–65°C. The temperature dependence, expressed in terms of the fluidity

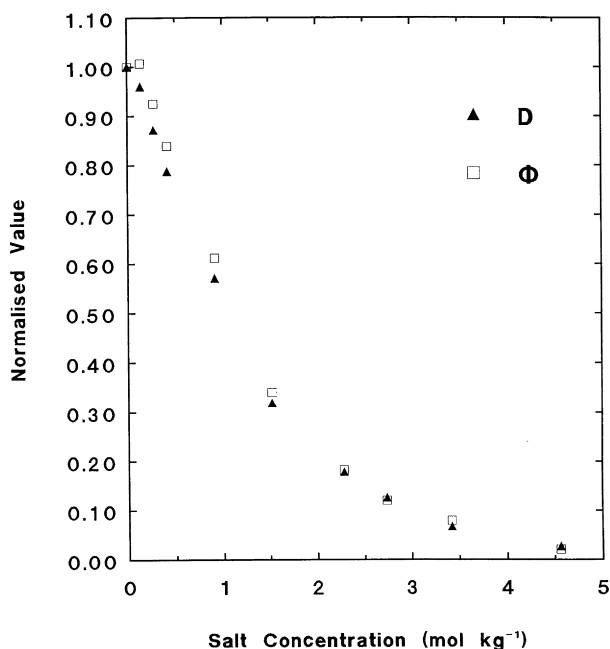


Fig. 9. Comparison of the behaviour of the fluidity and proton diffusion coefficient with salt concentration in DMF/LiT liquid electrolytes at 35°C. Each value has been normalized with respect to its value in unsalted DMF.

ϕ , fits very well to an Arrhenius equation:

$$\phi = \phi_0 \exp\left[-\frac{E_\phi}{RT}\right] \quad (7)$$

where ϕ_0 increases with increasing salt concentration, as does E_ϕ , which reflects increasing ion–ion and ion–solvent interactions. These results are shown in Fig. 7, with the activation energies given in Table 1.

Similar viscosity data for the TG/LiT electrolytes are shown in Fig. 8. There is, however, a difference from the DMF/LiT electrolytes in that the TG/LiT temperature dependence plots show curvature, suggesting that a Vogel–Tamman–Fulcher (VTF) type model [32–34] is appropriate so that:

$$\phi(T) = AT^{-1/2} \exp\left[-\frac{B}{T - T_0}\right] \quad (8)$$

Previous research [29] has suggested that for the TG systems, T_0 and A are constants, independent of salt concentration, whereas B (often referred to as a pseudo activation energy) increases linearly with increasing salt concentration.

In the case of proton diffusion coefficients, which are available over the entire concentration range in addition to the solvents themselves, their values may be normalized with respect to their values in the pure solvent, and these may be directly compared with normalized fluidity values. The results of the normalization at 35°C are given in Fig. 9 for the DMF/LiT electrolytes. There is good agreement in the behaviour of the proton diffusion and fluidity over the entire concentration range, giving an initial indication that the processes of solvent diffusion and viscous flow are related. Similar results have been obtained for the TG/LiT electrolytes.

To compare the behaviour of the diffusion of the ions with that of the fluidity (and further compare the solvent diffusion and fluidity) as the salt concentration changes, the natural logarithm of each of the proton, lithium and fluorine diffusion coefficients has been plotted against the natural logarithm of the viscosity at a temperature of 35°C. Fig. 10 shows this plot for the DMF/LiT electrolytes, with the plot for the TG/LiT systems shown in Fig. 11. If the Stokes–Einstein equation is valid in these systems, with a constant radius of diffusing species at all salt concentrations at 35°C, a gradient of +1 would be expected in the plots and this is indicated by the dotted lines on the figures. However, for both electrolytes the best linear fit to the plots (indicated by the solid lines) gives slightly shallower gradients for all diffusing species. This implies that either the measured viscosities are not a completely reliable measure of the ‘microscopic’ viscosity experienced by diffusing solvent molecules and ions, or that the effective radius of diffusing species is changing as the salt concentration of the electrolytes changes.

For both DMF/LiT and TG/LiT electrolytes, the temperature dependence of the diffusion coefficients and the fluidity

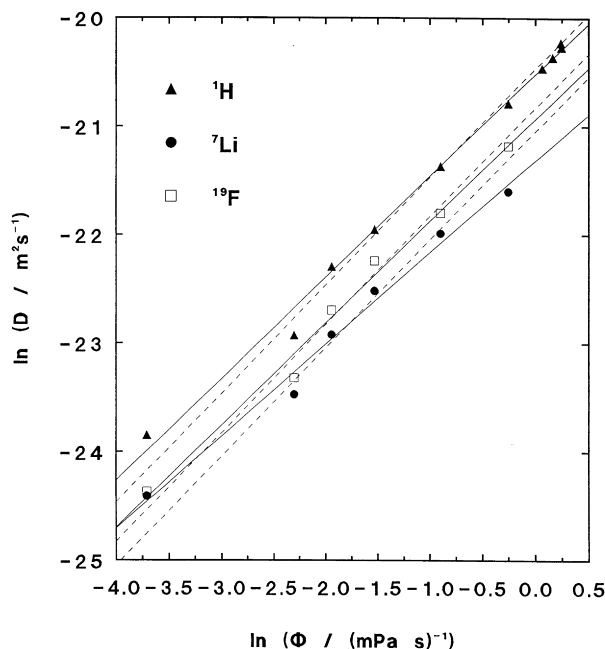


Fig. 10. Plot of the natural logarithm of the diffusion coefficient of protons, lithium and fluorine against the natural logarithm of the fluidity for DMF/LiT liquid electrolytes. The solid lines represent the best linear fits to the data and the dashed lines have a gradient of +1, predicted by the Stokes–Einstein equation.

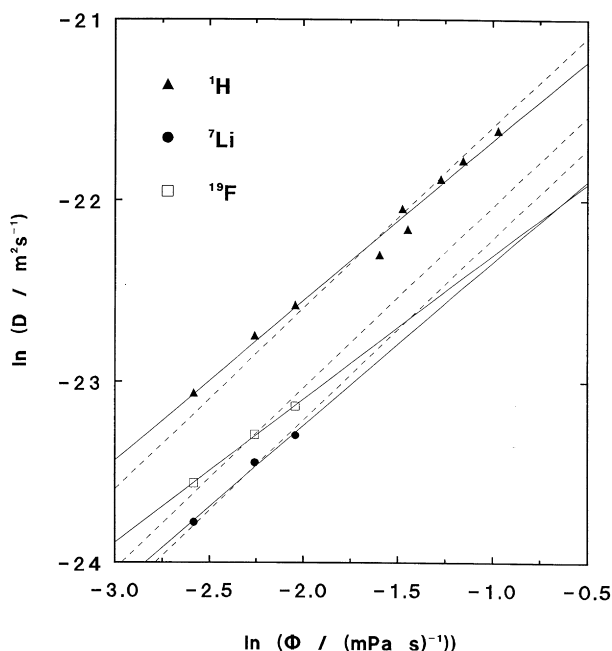


Fig. 11. Plot of the natural logarithm of the diffusion coefficient of protons, lithium and fluorine against the natural logarithm of the fluidity for TG/LiT liquid electrolytes. The solid lines represent the best linear fits to the data and the dashed lines have a gradient of +1, predicted by the Stokes–Einstein equation.

Table 3

Effective spherical radii of diffusing DMF molecules, Li^+ ions and CF_3SO_3^- ions in DMF/LiT electrolytes, calculated using experimental measurements of diffusion coefficient and viscosity in Eq. (6)

| O:Li | T/°C | Radius/Å | | |
|------|------|----------|---------------|----------------------------|
| | | DMF | Li^+ | CF_3SO_3^- |
| 3:1 | 35 | 1.34 | 2.35 | 2.26 |
| | 65 | 1.44 | 2.22 | 2.23 |
| 6:1 | 35 | 1.78 | 3.13 | 2.37 |
| | 65 | 1.75 | 2.99 | 2.35 |
| 15:1 | 35 | 1.87 | 4.20 | 2.77 |
| | 65 | 1.99 | 4.49 | 3.00 |
| DMF | 35 | 1.74 | — | — |
| | 65 | 1.64 | — | — |

can be compared. In the case of the DMF/LiT electrolytes, both the fluidity and diffusion of solvent molecules and ions exhibit Arrhenius-type temperature dependence and the activation energies obtained from the fits to the data can be directly compared.

The values of activation energies for diffusion and fluidity for DMF/LiT electrolytes, shown in Table 1, indicate that at low salt concentrations, the activation energy for proton diffusion is consistently higher than that of the fluidity. However, at high salt concentrations, the activation energies for the fluidity become very similar to the activation energies for the diffusion of DMF molecules (which we have already stated are reasonably similar to activation energies for the diffusion of anions and cations).

In contrast, the fluidity of the TG/LiT electrolytes has been found to be best modelled by a VTF-type equation over the temperature range studied, whereas the diffusion of all species is adequately fitted to an Arrhenius equation. However, if we restrict the temperature range of the fluidity measurements on the TG/LiT electrolytes to that of the n.m.r. diffusion measurements (as indicated in Fig. 8), the data can be very well described by a thermally activated process and very reasonable fits to Eq. (7) are obtained. Comparison of the activation energies for diffusion and fluidity over the restricted temperature range (Table 2) shows that the activation energies obtained from the fluidity data are again consistently lower by approx. 2–3 kJ/mol than those derived from the proton diffusion data.

It is therefore concluded that the activation energies associated with the processes of viscous flow and solvent diffusion are similar but not identical. This is not unexpected because the viscosity measurements relate to the bulk movement of the electrolyte solutions, whereas the diffusion measurements are sensitive to the movement of individual molecules over distances of the order of micrometres. There is also the related issue of the effective frequency of the macroscopic viscosity measurements compared with that relevant to the mobility of the solvent molecules and ions.

It is therefore with some reservations that we combine the viscosity measurements with the n.m.r. diffusion

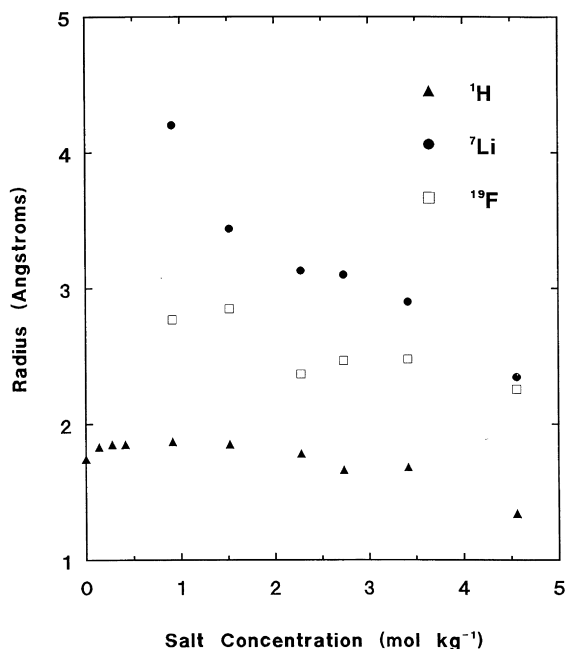


Fig. 12. Comparison of the effective radii of diffusing species in DMF/LiT liquid electrolytes. The radii were determined using experimental diffusion and viscosity data in the Stokes–Einstein equation.

coefficients in the Stokes–Einstein equation in order to calculate the effective radius of diffusing species in the liquid electrolytes and investigate the changes in its value with changing temperature and salt concentration.

For the DMF/LiT electrolytes the effective radii obtained for the various diffusing species at four salt concentrations at 35 and 65°C are summarized in Table 3. The values of a few Angstroms for the radius of a DMF molecule or a solvated ion are physically reasonable. Leng [35] estimated a radius of 2.65 Å for tetraglyme molecules in electrolyte solutions containing lithium perchlorate. Radii of 1.6 Å for propylene carbonate, 6.1 Å for Li⁺ and 3.1 Å for BF₄⁻ have

Table 4
Effective spherical radii of diffusing TG molecules, Li⁺ ions and CF₃SO₃⁻ ions in TG/LiT electrolytes, calculated using experimental measurements of diffusion coefficient and viscosity in Eq. (6)

| O:Li | T/°C | Radius/Å | | |
|------|------|----------|-----------------|--|
| | | TG | Li ⁺ | CF ₃ SO ₃ ⁻ |
| 12:1 | 35 | 1.77 | 3.61 | 2.91 |
| | 65 | 1.79 | 3.25 | 2.90 |
| | 80 | 1.81 | 3.17 | 2.89 |
| 15:1 | 35 | 1.79 | 3.59 | 3.08 |
| | 65 | 1.90 | 3.44 | 3.01 |
| | 80 | 1.90 | 3.62 | 2.89 |
| 18:1 | 35 | 1.87 | 3.83 | 3.26 |
| | 65 | 1.83 | 3.72 | 3.23 |
| | 80 | 1.78 | 3.63 | 3.03 |
| TG | 35 | 2.08 | — | — |
| | 65 | 2.08 | — | — |

been estimated [6] for constituents of propylene carbonate/LiBF₄ electrolytes at 27°C, salted to a concentration of 4.2% LiBF₄ by weight.

By examination of the effective radii of DMF molecules, cations and anions at 35 and 65°C (the two extreme temperatures at which both viscosity and diffusion measurements have been made) in Table 3, it appears that this change in temperature has no significant effect on the effective radii of any of the diffusing species.

The effect of salt concentration on the effective radii of DMF molecules, cations and anions at 35°C is shown in Fig. 12. Over the entire concentration range, the effective radii calculated for diffusing Li⁺ ions are noticeably larger than those calculated for diffusing CF₃SO₃⁻ ions, except at the highest salt concentration, where the two radii are very similar. There appears to be a general trend of a decrease in the effective radii of both ions as the salt concentration is increased, with the effect appearing to be the greatest for Li⁺ ions.

The higher diffusion coefficients measured for protons in comparison with fluorine and lithium is reflected in the lower effective radii calculated for diffusing DMF molecules compared with the radii of the anions and cations. It also appears that the effective radius of a diffusing DMF molecule is relatively unchanged over the entire range of salt concentrations studied, although at the highest salt concentrations (above approximately O:Li = 15:1), there is perhaps an indication of a slight fall in the radius as the salt concentration is increased. When the calculations of radii of DMF molecules at all the salt concentrations are considered it is found that the mean value is (1.78 ± 0.06) Å at 35°C and (1.81 ± 0.07) Å at 65°C.

The Stokes–Einstein equation has previously been applied to the proton diffusion and viscosity data for the TG/LiT electrolytes [36], where it was found that the effective radii of diffusing tetraglyme molecules was invariant to changes in both salt concentration and temperature. At 35°C the mean effective radius was found to be (1.94 ± 0.06) Å, and at 80°C the value was (1.99 ± 0.05) Å [36].

The Stokes–Einstein equation has now been used to estimate the effective radius of diffusing cations and anions, with the results at three temperatures summarized in Table 4, together with the calculated effective radii of TG molecules. Once again physically reasonable sizes of the order of a few Angstroms are calculated, with the effective radius of the cation generally being slightly larger than that of the anion at the same temperature and salt concentration. There is no real evidence in the values presented in Table 4 to suggest dramatic changes in the effective radii of diffusing cations or anions over the range of salt concentrations and temperatures investigated, although there is perhaps a slight trend towards the effective radii of both ions decreasing as the salt concentration increases. However, in view of the limited range of salt concentrations available for n.m.r. measurements, it should be noted that this observation could be simply the result of uncertainties in measured viscosities

and diffusion coefficients, and therefore no great significance should be made of this.

It is, however, perhaps a little surprising that the effective radius of tetraglyme, which is a reasonably large solvent molecule, is of the order of 1.5–2 times smaller than the effective radius of diffusing anions and cations. This is consistent with the idea of ‘free’ tetraglyme molecules contributing to the proton diffusion measurements (even at levels of salt concentration approaching the saturation limit), with the larger effective radius of ions accounted for by a (partially) complete solvation shell which comprises tetraglyme molecules. The slightly larger effective radius of cations compared with anions may reflect a stronger attraction of tetraglyme molecules to Li^+ compared with CF_3SO_3^- .

3.5. Comparison with other techniques

Patterns in ionic association in the DMF/LiT and TG/LiT liquid electrolytes have previously been reported using Raman spectroscopy measurements [37] and ‘Walden product’ interpretations [10,29].

In the case of the Raman measurements, up to three components of the symmetric stretch of the SO_3^- unit of the CF_3SO_3^- anion were observed. These components were attributed to free anions, contact ion pairs and higher order aggregates, with their relative concentrations determined by an analysis of the area of their respective peaks.

The ‘Walden product’ is the product of the molal conductivity, Λ , and viscosity η of an electrolyte [27]. Combination of the Stokes–Einstein and Nernst–Einstein equations leads to the relationship:

$$\Lambda\eta \propto \frac{\delta e^2}{6\pi a} \quad (9)$$

where δ is the fractional salt dissociation ($\delta \propto n/m$). Therefore, the Walden product is proportional to the fractional salt dissociation.

The Raman results for the DMF/LiT electrolytes at a temperature of 20°C indicate that contact ion pairs form at salt concentrations of 18:1 and above, with higher aggregates forming at salt concentrations above 5:1. The proportion of ions in contact ion pairs increases with increasing salt concentration, which is consistent with the observed rise in Δ as the salt concentration is increased. At a concentration of 3:1, 60% of ions are accounted for in the form of contact ion pairs, which is in good agreement with the value $\Delta = 0.70$, that was calculated for the 3:1 electrolyte at a temperature of 35°C.

An observed fall in the Walden product with increasing salt concentration also indicates that there is less dissociation of the salt as the salt concentration is increased in DMF/LiT electrolytes, although the results also provide evidence of a levelling off in the fractional dissociation at concentrations above approximately 5:1. This effect at higher salt concentrations could, however, be due to a fall in the

effective radii of diffusing cations and anions, suggested by the Stokes–Einstein equation or the measured viscosities at higher salt concentrations deviating further away from the ‘microscopic’ viscosity experienced by the diffusing ions.

At salt concentrations of 6:1 and 4:1, the Walden product and Raman results indicate a fall in the free ion fraction as the temperature increases from 25 to 80°C. For this temperature increase the fall in the free ion fraction was 23% and the Walden product fell by 33% for the 6:1 DMF/LiT solution; at a concentration of 4:1, the free ion fraction and Walden product fell by 24 and 23%, respectively. This can be compared with the fall in $(1-\Delta)$ for a temperature rise from 35 to 80°C, which is calculated to be 13% for the 6:1 electrolyte and 16% for the 4:1 electrolyte.

We can also compare the trends in Δ for the TG/LiT electrolytes to the experimental evidence provided by Raman spectroscopic studies and Walden product interpretations. The Raman studies at 45°C show that the free ion fraction is constant for low salt concentrations up to approximately 30:1, where the free ion fraction falls then levels off again at around 0.2. At this salt concentration there is a corresponding increase in the proportion of ions present in contact pairs, which then remains approximately constant at a value of 0.7. Higher ionic aggregates are only observed at salt concentrations of 15:1 and 12:1, but then only at a fractional content of less than 0.1. Throughout the entire concentration range, the Walden product is observed to rise linearly with increasing salt concentration, which is in good agreement with the fall in Δ with increasing salt concentration.

The behaviour with temperature for the TG/LiT electrolytes is qualitatively the same for $(1-\Delta)$, the Raman free ion fraction and the Walden product. As the temperature is increased from 25 to 80°C, the free ion fraction falls by 33% for the 12:1 salt concentration and the Walden product falls by 21%. At the same concentration, $(1-\Delta)$ falls by 19% as the temperature rises from 35 to 80°C.

Therefore, we can identify that for both DMF/LiT and TG/LiT electrolytes, the Walden product, Raman measurements and Λ calculations are all, at least qualitatively, in agreement that there is increased ionic association as the temperature increases. There is also qualitative agreement between the three measures of ionic association with changing salt concentration for the DMF/LiT electrolytes. However, there are some differences in the behaviour of the three measures with changing salt concentration for the TG/LiT electrolytes. The Walden product and Λ calculations both suggest that there is greater association as the salt concentration decreases. In contrast, the Raman measurements indicate an overall trend of an increasing number of ion pairs with increasing salt concentration, although it should be noted that there is very little change in the ionic composition of the electrolytes indicated by these measurements over the range of salt concentrations covered by the n.m.r. lithium and fluorine diffusion measurements.

This highlights some of the concerns regarding Raman measurements on electrolyte systems. The Raman measurements are sensitive to the relative proximity of the anions and cations, whereas the n.m.r. measurements independently measure the diffusion of the ions over distances of the order of micrometres. Gray [38] points out that at high levels of salt concentration, packing considerations mean that there is significant anion–cation contact which will affect the Raman measurements, although ionic interactions are likely to involve correlated motions in addition to the formation of discrete ion pairs. In addition, Boden et al. [7] and Torrell et al. [14] have both suggested that the timescale of the Raman measurements (picoseconds) may be too short to probe ion–ion interactions which are of sufficient duration to affect the ionic conductivity of an electrolyte.

4. Conclusions

The diffusion coefficients of solvent molecules, Li^+ and CF_3SO_3^- ions in electrolyte solutions of TG/LiT and DMF/LiT over a range of salt concentrations and temperatures have been measured using PFG n.m.r. In both electrolytes the solvent diffusion coefficient is always greater than either the cation or anion diffusion coefficient, reflecting a contribution from ‘free’ solvent molecules. The value of the diffusion coefficient for CF_3SO_3^- ions in both electrolytes is, in turn, always greater than that for Li^+ ions, although at the highest salt concentrations the two become almost coincident, representing an increase in ionic association or correlated motion of the ions.

The issue of ionic association was probed using the ionic conductivity and diffusion data in the Nernst–Einstein equation. For both electrolytes, ionic association is seen to increase with increasing temperature, which is consistent with previous results from Raman spectroscopy measurements and Walden product interpretations. However, ionic association is seen to increase with increasing salt concentration for the DMF/LiT electrolytes but to decrease for the TG/LiT electrolytes. The behaviour of the DMF/LiT electrolytes is typical of ‘strong’ electrolytes, whereas the TG/LiT electrolytes at high levels of salt concentration are better described as ionic melts.

Correlations between the macroscopic property of fluidity and the microscopic property of diffusion have been obtained, with small deviations from the Stokes–Einstein equation with salt concentration and temperature being attributed to the very different length and time scales over which the measurements were taken.

References

- [1] Voice AM, Southall JP, Rogers V, Matthews KH, Davies GR, McIntyre JE, Ward IM. *Polymer* 1994;35(16):3363.
- [2] McIntyre JE, Ward IM, Hubbard HVStA, Rogers V. UK Patent GB2260137, 1993.
- [3] Stejskal EO, Tanner JE. *J Chem Phys* 1965;42:288.
- [4] Mills R. *J Phys Chem* 1973;77:687.
- [5] Kaye GWC, Laby TH. *Tables of physical and chemical constants*. New York: Longman, 1973.
- [6] Clericuzio M, Parker Jr WO, Soprani M, Andrei M. *Sol St Ion* 1995;82:179.
- [7] Boden N, Leng SA, Ward IM. *Sol St Ion* 1991;45:261.
- [8] Ward IM, Boden N, Cruickshank J, Leng SA. *Electrochem Acta* 1995;40(13-14):2071.
- [9] Jost W. *Diffusion*. New York: Academic Press, 1960.
- [10] Southall JP, Hubbard HVStA, Johnston SF, Rogers V, Davies GR, McIntyre JE, Ward IM. *Sol St Ion* 1996;85:51.
- [11] Cruickshank JM. Ph.D. Thesis, Dept. of Physics, University of Leeds, 1993.
- [12] Schantz S, Torrell LM, Stevens JR. *J Chem Phys* 1991;94(10):6862.
- [13] Peterson G, Jacobsson P, Torrell LM. *Electrochem Acta* 1992;37(9):1495.
- [14] Torrell LM, Jacobsson P, Peterson G. *Polym Adv Technol* 1993;4:152.
- [15] Benson A, Lindgren J. *Sol St Ion* 1993;60:37.
- [16] Peterson G, Torrell LM, Panero S, Scrosati B, da Silva CJ, Smith M. *Sol St Ion* 1993;60:55.
- [17] Olender R, Nitzan A. *Electrochem Acta* 1995;40:1505.
- [18] Ratner MA, Nitzan A. *Faraday Discuss Chem Soc* 1989;88:19.
- [19] Forsyth M, Payne VA, Ratner MA, de Leeuw SW, Shriver DF. *Sol St Ion* 1992;53:1011.
- [20] Popovych O, Tomkins RPT. *Nonaqueous solution chemistry*. Chichester, UK: Wiley, 1981.
- [21] Cisak A, Werblan L. *High energy non-aqueous batteries*. Ellis Horwood, 1993.
- [22] MacCallum JR, Tomlin AS, Vincent CA. *Eur Polym J* 1986;22(10):787.
- [23] Cameron GG, Ingram MD, Sorrie SA. *J Chem Soc Faraday Trans 1* 1987;83:3345.
- [24] Hall PG, Davies GR, Ward IM, McIntyre JE. *Polym Commun* 1986;27:100.
- [25] Fuoss RM, Kraus CA. *J Am Chem Soc* 1933;55(2):2387.
- [26] Gestblam B, Songstad J. *Acta Chem Scand* 1987;B41:396.
- [27] Bockris JO'M, Reddy AKN. *Modern electrochemistry*, vol. 1. New York: Plenum Press, 1970.
- [28] Bruce PG, Vincent CA. *J Chem Soc Faraday Trans* 1993;89(17):3187.
- [29] Southall JP. Ph.D. Thesis, Dept. of Physics, University of Leeds, 1995.
- [30] Robbins J. *Ions in solution (2)*. Oxford: Clarendon Press, 1972.
- [31] Marcus Y. *Ion solvation*. Chichester: Wiley, 1985.
- [32] Vogel H. *Phys Z* 1921;22:645.
- [33] Tamman G, Hesse W. *Z Anorg Allg Chem* 1926;156:245.
- [34] Fulcher GS. *J Am Ceram Soc* 1925;8:339.
- [35] Leng SA. Ph.D. Thesis, Dept. of Physics, University of Leeds, 1988.
- [36] Williamson MJ, Southall JP, Hubbard HVStA, Johnston SF, Davies GR, Ward IM. *Electrochem Acta* 1998;43:1415.
- [37] Johnston SF, Ward IM, Cruickshank J, Davies GR. *Sol St Ion* 1996;90:39.
- [38] Gray FM. *Solid polymer electrolytes: fundamentals and technological applications*. VCH, 1991.